

## Cyanide-free silver electroplating process in thiosulfate bath and microstructure analysis of Ag coatings

Feng-zhang REN<sup>1</sup>, Li-tao YIN<sup>1</sup>, Shan-shan WANG<sup>2</sup>, A. A. VOLINSKY<sup>3</sup>, Bao-hong TIAN<sup>1</sup>

1. School of Materials Science and Engineering, Henan University of Science and Technology, Luoyang 471023, China;
2. Luoyang Bearing Science and Technology Corporation Limited, Luoyang 471039, China;
3. Department of Mechanical Engineering, University of South Florida, Tampa, FL 33620, USA

Received 29 October 2012; accepted 23 December 2012

**Abstract:** Cyanide-free silver electroplating was conducted in thiosulfate baths containing AgNO<sub>3</sub> and AgBr major salts, respectively. The effects of major salt content and current density on surface quality, deposition rate and microhardness of Ag coatings were investigated. The optimized electroplating parameters were established. The adhesion strength of Ag coating on Cu substrate was evaluated and the grain size of Ag coating was measured under optimized electroplating parameters. The optimized AgNO<sub>3</sub> content is 40 g/L with current density of 0.25 A/dm<sup>2</sup>. The deposited bright, smooth, and well adhered Ag coating had nanocrystalline grains with mean size of 35 nm. The optimized AgBr content was 30 g/L with current density of 0.20 A/dm<sup>2</sup>. The resultant Ag coating had nanocrystalline grains with mean size of 55 nm. Compared with the bath containing AgBr main salt, the bath containing AgNO<sub>3</sub> main salt had a wider current density range, and corresponding Ag coating had a higher microhardness and a smaller grain size.

**Key words:** cyanide-free silver electroplating; thiosulfate; current density; bonding strength; grain size

### 1 Introduction

Cyanide-based silver-plating solutions are widely used in electroplating industry because they offer most consistent deposition quality at the lowest cost. Due to environmental concerns, cyanide-based process must be replaced with the cyanide-free silver-plating solution [1,2]. There are multiple studies of cyanide-free silver electroplating process. The best results have been obtained using iodide or thiosulfate as ligands. Of these, however, only the thiosulfate bath has succeeded in attaining any technical importance, albeit negligible, owing to its limited stability. In 1976, CULJKOVIE [3] improved a thiosulfate bath. The improved thiosulfate bath has the throwing power almost the same as that of cyanide bath, and the prepared silver coating in the improved bath is bright with good anti-tarnish property. In the same year, LEAHY and KARUSTIS [4] added hydrosulphite buffer, sulphate and other additives in the thiosulfate bath, and thus obtained better bath stability. In 1989, SRIVEERARAGHAVAN et al [5] reported a

thiosulfate bath with several months' stability, and high adhesion strength of silver coating electroplated on copper substrates. However, in these references, coating appearance was not mentioned.

In 1994, NOBEL et al [6] proposed an electroplating solution, which contained at least a monovalent metal, thiosulfate ions, and a stabilizer of organic sulfinate compound. However, the resistance to discoloration of this coating was poor. In 1996, JAYAKRISHNAN et al [7] provided an information on a silver plating solution based on a succinimide complex. However, the deposit was not bright and no data on adhesion strength was reported. In 2005, SU et al [8] optimized the cyanide-free silver pulse plating processes, although the anti-tarnish treatment was rather complex. In 2008, ANASTASSAKIS and SEQUEIRA [9] investigated the appropriateness of thiosulphate as an alternative for cyanide in electroplating baths. ABBOTT et al [10] demonstrated that a sustained galvanic coating of silver can be deposited onto copper substrates from a solution of Ag ions in an ionic liquid based on a chlorine chloride eutectic. In 2009, XIE et al [11] proposed a cyanide-free

silver electroplating solutions containing uracil, but the silver plating bath was relatively complex. In 2011, FISHELSON et al [12] prepared silver films from near to neutral non-cyanide solution. Mirror-quality bright and white Ag coatings were obtained from proprietary Ag plating bath. However, they did not mention coatings adhesion strength [9,10,12].

Unfortunately, silver deposits obtained using these non-cyanide electrolytes were of a lesser quality than those obtained with traditional cyanide electrolytes [13]. To our knowledge, there is no commercially available non-cyanide silver plating process that meets all desired requirements regarding the solution and the silver deposit quality. Thus, cyanide-free silver electroplating needs to be further studied and improved for wider industrial use.

To further explore the cyanide-free silver plating and optimize the silver plating solution in present work, the cyanide-free silver electroplating was conducted in thiosulfate baths containing  $\text{AgNO}_3$  or  $\text{AgBr}$  main salts. The effects of major salt content and current density on surface quality, deposition rate and microhardness of Ag coatings were investigated. Electroplating parameters were optimized. The adhesion strength of Ag coating on Cu substrate was evaluated and the grain size of Ag coating was measured under the optimal process conditions.

## 2 Experimental

### 2.1 Cathode substrate pre-treatment

Copper sheets with purity of 99.97%–99.99% (mass fraction) and size of 35 mm×25 mm×1.5 mm were used as cathode substrates. The substrates were mechanically polished, washed from oil in hot aqueous alkali and acetone, and placed into 10% (volume fraction) hydrochloric acid solution for 8–10 s for surface activation. The samples were then placed in the galvanic bath for electroplating.

### 2.2 Bath preparation and maintenance

#### 2.2.1 $\text{AgNO}_3$ solution system

Sodium hyposulfite ( $\text{Na}_2\text{S}_2\text{O}_3$ ) was dissolved in distilled water to a third of the bath volume. Silver nitrate ( $\text{AgNO}_3$ ) and potassium metabisulfite ( $\text{K}_2\text{S}_2\text{O}_5$ ) were dissolved in distilled water to a quarter of the bath volume, respectively.  $\text{K}_2\text{S}_2\text{O}_5$  solution was poured into  $\text{AgNO}_3$  stirred solution to form potassium metabisulfite ( $\text{Ag}_2\text{S}_2\text{O}_5$ ) turbid solution. The turbid solution was slowly added to  $\text{Na}_2\text{S}_2\text{O}_3$  solution to turn it into yellowish clear liquid. Appropriate amount of ammonium acetate ( $\text{CH}_3\text{COONH}_4$ ) was added to the solution and left for a short time. Amino thiourea ( $\text{CH}_5\text{N}_3\text{S}$ ) was then completely dissolved in the solution. Finally, distilled water was added to top up the bath.

Bath composition changes due to long

electroplating time, and impurities are carried into the bath by the cathode. Bath composition needs to be checked and adjusted, and impurities need to be removed. In this test, when the accumulative electroplating time lasted for 20 h, composition check and adjustment were carried out. It is suitable for keeping the mass ratio of  $\text{AgNO}_3:\text{K}_2\text{S}_2\text{O}_5:\text{Na}_2\text{S}_2\text{O}_3$  at about 1:1:5.  $\text{AgNO}_3$  and  $\text{K}_2\text{S}_2\text{O}_5$  should be added at the same time at ratio of 1:1.  $\text{AgNO}_3$  should not be added in  $\text{Na}_2\text{S}_2\text{O}_3$  solution directly to avoid precipitation of black  $\text{Ag}_2\text{S}$ . Solution pH value of about 5.8 was maintained by adding acetic acid.

#### 2.2.2 $\text{AgBr}$ solution system

Sodium hyposulfite ( $\text{Na}_2\text{S}_2\text{O}_3$ ) was dissolved in distilled water to two thirds of the bath volume. Sodium sulfite ( $\text{Na}_2\text{SO}_3$ ), ammonium acetate ( $\text{CH}_3\text{COONH}_4$ ), silver bromide ( $\text{AgBr}$ ) and amino thiourea ( $\text{CH}_5\text{N}_3\text{S}$ ) were sequentially dissolved in the same solution. Finally, distilled water was added to the solution to top up the bath, and the solution pH value was adjusted to about 6.5 by adding acetic acid. The bath also had to be filtered periodically (accumulative electroplating time of 20 h) in order to remove the impurities carried in by the cathode.

## 2.3 Electroplating process

The anode was 99.9% (mass fraction) pure silver plate and the cathode was a pre-treated copper sheet. Electroplating process parameters of  $\text{AgNO}_3$  and  $\text{AgBr}$  solution systems are listed in Table 1. Coating thickness was controlled by electroplating duration at different current densities.

**Table 1** Electroplating process parameters of  $\text{AgNO}_3$  and  $\text{AgBr}$  electroplating solution systems

Parameter	$\text{AgNO}_3$ system	$\text{AgBr}$ system
$\rho(\text{AgNO}_3)/(\text{g}\cdot\text{L}^{-1})$	30–50	–
$\rho(\text{AgBr})/(\text{g}\cdot\text{L}^{-1})$	–	20–40
$\rho(\text{Na}_2\text{S}_2\text{O}_3)/(\text{g}\cdot\text{L}^{-1})$	225	200
$\rho(\text{K}_2\text{S}_2\text{O}_5)/(\text{g}\cdot\text{L}^{-1})$	40	–
$\rho(\text{Na}_2\text{SO}_3)/(\text{g}\cdot\text{L}^{-1})$	–	50
$\rho(\text{CH}_3\text{COONH}_4)/(\text{g}\cdot\text{L}^{-1})$	25	40
$\rho(\text{CH}_5\text{N}_3\text{S})/(\text{g}\cdot\text{L}^{-1})$	0.6–0.8	0.2–0.5
pH value	5.5–6.0	6.3–6.8
Current density/ $(\text{A}\cdot\text{dm}^{-2})$	0.1–0.3	0.1–0.3

## 2.4 Post-treatment for anti-tarnishing

In order to avoid discoloration of the silver coating in air, the following treatments were carried out. Silver plated part was in turn immersed in concentrated hydrochloric acid (35%–38%) for 30 min, in 60 g/L  $\text{Cr}_2\text{O}_3$  and 16 g/L NaCl water solution for 8–10 s, in 200 g/L  $\text{Na}_2\text{S}_2\text{O}_3$  water solution for 3–5 s, in 100 g/L NaOH water solution for 5–8 s, and in concentrated hydrochloric acid for 10–15 s. Whenever plated part was

taken out from a solution, it was immediately washed with water.

## 2.5 Coating characterization and microstructure observations

### 2.5.1 Microstructure observation and deposition rate measurement

Surface morphology observation and deposition rate measurements at different current densities of silver coating were carried out using scanning electron microscopy (SEM, JSM-5610LV). The deposition rate is the ratio of the coating thickness and the corresponding deposition time. Because of the edge effect, the deposit roughness and the deposition rate at the substrate edges are larger than those in the centers, thus the surface morphology observations and the deposition rate measurements were performed in the middle of the specimen surface.

### 2.5.2 Hardness measurements

The coating hardness was measured using a microhardness tester. The load and hold time were 0.49 N and 15 s, respectively. The mean value of hardness measured from seven micro-areas per sample was taken. Finite element analysis revealed that the hardness value for a thin metal film was not influenced by the substrate when the indentation depth was smaller than one tenth of the film thickness [14]. To obtain coating hardness not influenced by the substrate, the indentation depth was kept 10 times less than the coating thickness.

### 2.5.3 Adhesion strength evaluation

Two methods outlined in the QB/T 3821–1999 Light Industry Standard of the People's Republic of China were used to evaluate the coating adhesion strength. One method included drawing a 1 mm side square on the coating surface using a knife. Whether the coating flaked off the substrate was used to distinguish between good and bad adhesion. The other method consisted of bending the sample repeatedly until it broke, and whether the coating flaked off or crackled was used to characterize the coating adhesion strength.

### 2.5.4 Grain size and texture analysis

The crystallites size perpendicular to the  $(hkl)$  crystalline plane can be calculated using the Scherrer equation  $D_{(hkl)} = k\lambda(\beta\cos\theta)^{-1}$ . In the equation,  $k$  is the Scherrer constant ( $k=0.89$ );  $D_{(hkl)}$  is the crystallites size perpendicular to the crystalline plane (nm);  $\beta$  is the full width at half maximum of the strongest diffraction reflection of the  $(hkl)$  crystalline plane (rad);  $\theta$  is the diffraction angle of the strongest diffraction reflection of the  $(hkl)$  crystalline plane ( $^{\circ}$ );  $\lambda$  is the length of X-ray wave (nm).

Typically electroplated metal coatings are nanocrystalline, so grain size can be measured using the X-ray diffraction method. In Ref. [15], the electroplated

Ni coatings grain size was measured by means of X-ray diffraction and metallography with good matching. The phases and texture of the Ag coatings were analyzed, and the grain sizes were measured using a BRUKER D8 X-ray diffractometer. A Cu target was used with corresponding X-ray wave length of 0.154056 nm.

Texture coefficient ( $C$ ) of a crystalline plane characterizes the degree of the crystal plane preferred orientation. For  $(hkl)$  crystal plane,  $C_{(hkl)}$  can be written as [16]

$$C_{(hkl)} = \frac{I_{(hkl)}/I_{0(hkl)}}{\sum_{i=1}^n I_{(h_i k_i l_i)}/I_{0(h_i k_i l_i)}} \times 100\% \quad (1)$$

where  $I_{(hkl)}$  and  $I_{0(hkl)}$  are the diffraction intensities of  $(hkl)$  crystal plane of the deposited sample and the standard powder sample, respectively;  $n$  is the number of crystalline planes with relatively high diffraction intensity. If  $C$  value of every crystalline plane is the same, preferred orientation is not present.

## 3 Results and discussion

### 3.1 Effect of main salt on silver coating surface quality

With current densities of 0.25 and 0.20 A/dm<sup>2</sup> for AgNO<sub>3</sub> and AgBr solution systems, respectively, the effects of main salt contents on surface quality of silver coating are listed in Table 2. As shown in Table 2, when the main salt contents are 40 g/L and 45 g/L for AgNO<sub>3</sub> and 30 g/L and 35 g/L for AgBr, respectively, the silver coatings are bright. Considering surface quality and bath cost, 40 g/L AgNO<sub>3</sub> for AgNO<sub>3</sub> solution system and 30 g/L AgBr for AgBr solution system should be adopted in the following tests.

**Table 2** Effects of main salt content on surface quality of silver coating

AgNO <sub>3</sub> system $\rho(\text{AgNO}_3)/(\text{g}\cdot\text{L}^{-1})$	Surface quality	AgBr system, $\rho(\text{AgBr})/(\text{g}\cdot\text{L}^{-1})$	Surface quality
30	Yellow	20	Yellow
35	Semi-bright	25	Semi-bright
40	Bright	30	Bright
45	Bright	35	Bright
50	Rough, nigrescent	40	Rough, nigrescent

### 3.2 Effect of current density on silver coating surface quality

The surface quality of coatings prepared at different current densities is shown in Table 3. The surface morphologies of coatings prepared at different current

densities for two solution systems are shown in Figs. 1 and 2, respectively. In Fig. 1, the surfaces of coatings are flat at different current densities. The surface is slightly rough at the maximum current density of  $0.3 \text{ A/dm}^2$  compared to other current densities. In Fig. 2, the surfaces of coatings are flat at moderate current densities. The surfaces are uneven at the minimum and maximum current density.

**Table 3** Surface quality of coatings prepared at different current densities

Current density/ $(\text{A}\cdot\text{dm}^{-2})$	$\text{AgNO}_3$ system	$\text{AgBr}$ system
0.10	Yellow	Yellow
0.15	Semi-bright	Semi-bright
0.20	Semi-bright	Bright
0.25	Bright	Semi-bright
0.30	Rough, nigrescent	Rough, nigrescent

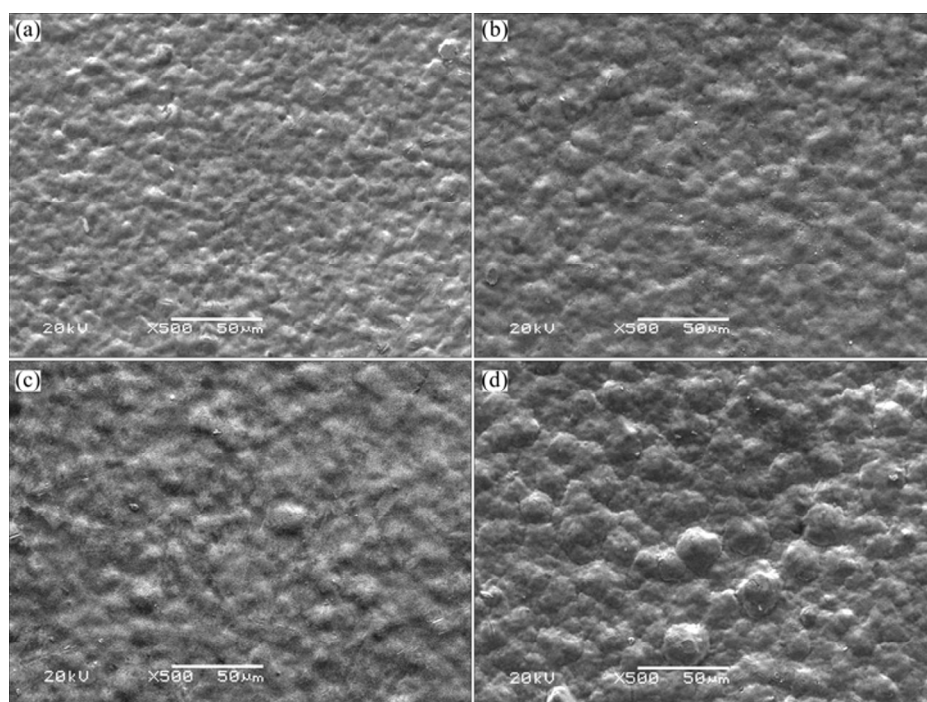


**Fig. 1** Surface morphologies of silver coating prepared at different current densities for  $\text{AgNO}_3$  solution system: (a)  $0.10 \text{ A/dm}^2$ ; (b)  $0.20 \text{ A/dm}^2$ ; (c)  $0.25 \text{ A/dm}^2$ ; (d)  $0.30 \text{ A/dm}^2$

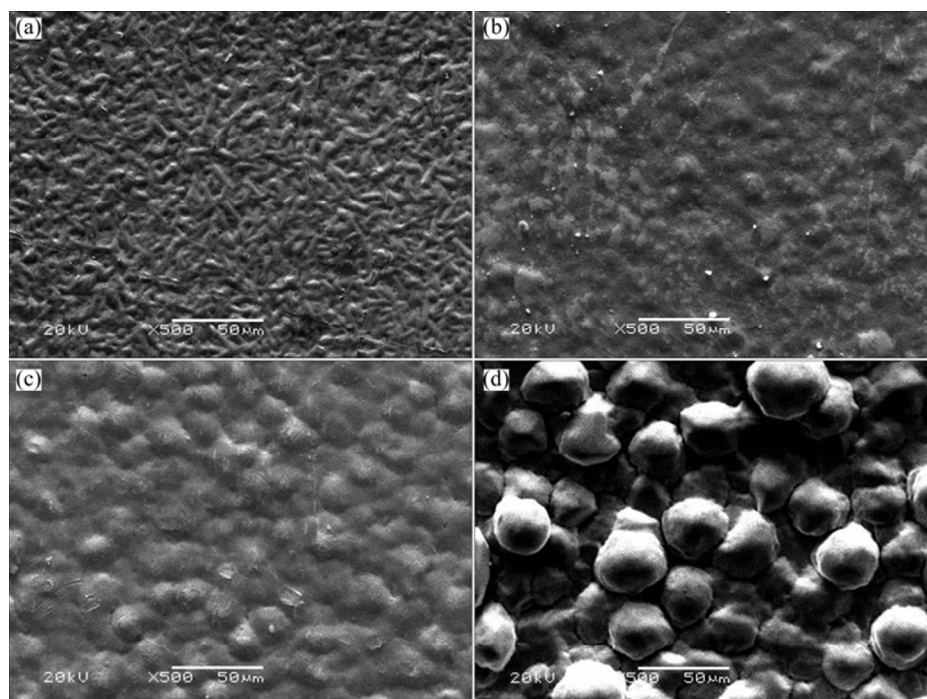


**Fig. 2** Surface morphologies of silver coating prepared at different current densities for  $\text{AgBr}$  solution system: (a)  $0.10 \text{ A/dm}^2$ ; (b)  $0.15 \text{ A/dm}^2$ ; (c)  $0.20 \text{ A/dm}^2$ ; (d)  $0.25 \text{ A/dm}^2$

The above phenomena can be explained as follows. The deposition rate increases with the current density increasing. The increase of current density leads to the increase of the overpotential, therefore, results in the increase of nucleation rate. When the current density is relatively small, the nucleation rate is low. The lower nucleation rate provides the crystal nucleus with a larger space to grow, which results in the formation of an uneven surface. The increase of nucleation rate with the current density will make many crystal nuclei grow synchronously and, therefore, results in the formation of a flat surface. When the current density is too high, micro-discharge usually occurs at a sharp angle due to the lack of discharge metallic ions near the cathode, which causes larger grains and surface coarsening.

Moreover, from Figs. 1 and 2, it can be seen that the effects of current density on surface morphology of coatings for AgBr solution system are more obvious than that for AgNO<sub>3</sub> solution system, which indicates that adaptable current density range for the AgNO<sub>3</sub> solution system is wider than that for the AgBr solution system.

As shown in Table 3, Figs. 1 and 2, the optimal current densities for AgNO<sub>3</sub> and AgBr solution systems are 0.25 A/dm<sup>2</sup> and 0.20 A/dm<sup>2</sup>, respectively.

### 3.3 Adhesion of silver coatings

Adhesion of silver coatings was tested using above mentioned two methods. Both silver coatings, which were prepared at 40 g/L AgNO<sub>3</sub> and 0.25 A/dm<sup>2</sup> for AgNO<sub>3</sub> solution system and at 30 g/L AgBr and 0.20 A/dm<sup>2</sup> for AgBr solution system, respectively, did not flake off the substrate or crack. This indicated good adhesion between the coating and the substrate.

### 3.4 Effects of current density on deposition rate and hardness

The deposition rates of the two systems at different current densities are shown in Fig. 3. As the current density increases, the deposition rate of both systems increases. The deposition rate of the AgNO<sub>3</sub> system is greater than that of the AgBr system at the same current density, except the current density of 0.25 A/dm<sup>2</sup>. At 0.25 A/dm<sup>2</sup>, the coating surface of the AgBr system is very rough, whereas the coating surface of AgNO<sub>3</sub> system is relatively smooth, which causes the measured deposition rate of the AgBr system to be higher than its true deposition rate. The measured deposition rate of the AgNO<sub>3</sub> system is close to its true deposition rate. This is why the measured deposition rate of the AgBr system is slightly higher than that of the AgNO<sub>3</sub> system at 0.25 A/dm<sup>2</sup>.

Figure 4 shows the relationship between the current density and the hardness of silver coatings. With the increase of the current density, the microhardness of

silver coatings of both systems originally increases and then decreases, although the hardness does not change much. The coatings at the current density of 0.2 A/dm<sup>2</sup> for both solution systems have a higher hardness because the coatings surface is relatively even and dense. The microhardness of the AgNO<sub>3</sub> system is lower than that of the AgBr system for the same current density.

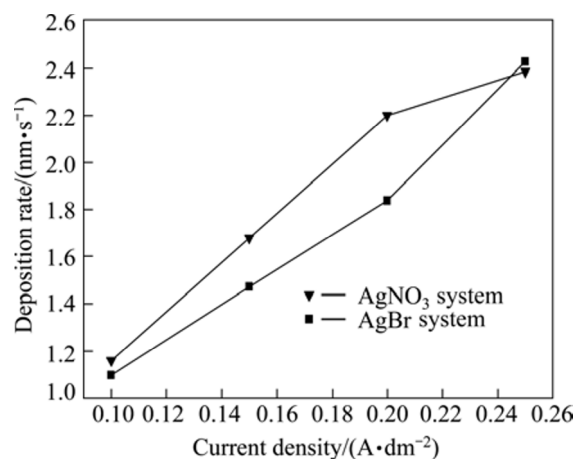


Fig. 3 Deposition rates at different current densities

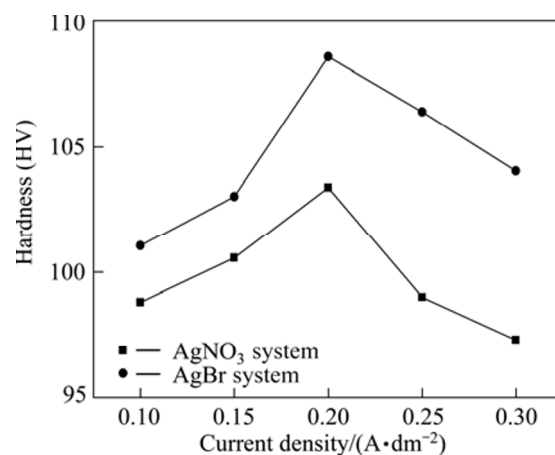


Fig. 4 Relationship between current density and microhardness

The XRD patterns of silver coatings prepared for the AgNO<sub>3</sub> system at 0.25 A/dm<sup>2</sup> current density are shown in Fig. 5, and for the AgBr system at 0.20 A/dm<sup>2</sup> current density in Fig. 6. The average grain sizes, calculated from the (111), (200), (220), (311) and (222) reflections, are 35 nm for the AgNO<sub>3</sub> system and 55 nm for the AgBr system, respectively.

In Fig. 5, the strongest diffraction reflection appears at 2θ of about 64°, and corresponds to the (220) silver crystalline plane. Silver coating from the AgNO<sub>3</sub> system has (220) preferred orientation. Based on Fig. 6, the silver coating from the AgBr system has (220) and (111) preferred orientations with relatively higher (111) preferred orientation.

Generally speaking, when the grain size is smaller than the limiting grain size with stable dislocations, the

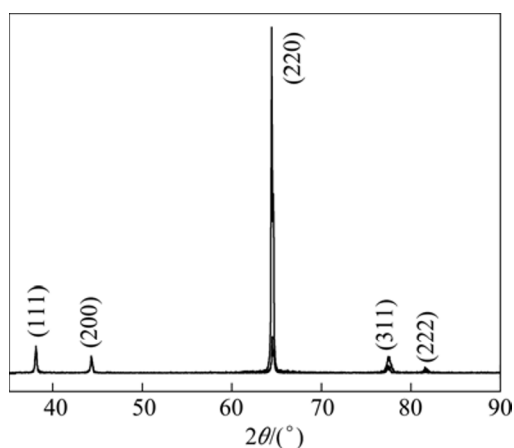


Fig. 5 XRD pattern of silver coating from  $\text{AgNO}_3$  system

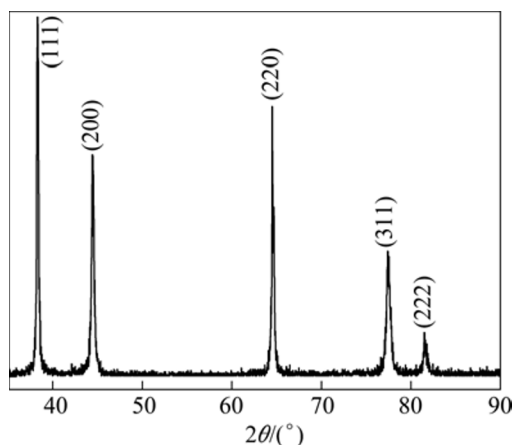


Fig. 6 XRD pattern of silver coating from  $\text{AgBr}$  system

hardness will increase with the decrease of grain size [17]. The calculated limiting size of Ag is 27 nm [17]. Based on this, the hardness Ag coating of from the  $\text{AgNO}_3$  system with 35 nm grains should be higher than that from the  $\text{AgBr}$  system with 55 nm grains. In reality, the silver coating from  $\text{AgBr}$  solution displays higher hardness. This may be due to the internal stress and/or surface roughness of both coatings.

#### 4 Conclusions

1) For the  $\text{AgNO}_3$  system, the optimal current density is  $0.25 \text{ A/dm}^2$  and the  $\text{AgNO}_3$  main salt content is 40 g/L. Under these conditions, the prepared coating is bright and flat, and the average grain size is 35 nm.

2) For the  $\text{AgBr}$  system, the optimal current density is  $0.20 \text{ A/dm}^2$  and the main  $\text{AgBr}$  salt content is 30 g/L. Under these conditions, the prepared coating is bright and flat, and the average grain size is 55 nm. Compared with the  $\text{AgBr}$  system, the  $\text{AgNO}_3$  system is better suited for electroplating with a wider current density range, higher coating microhardness, and smaller grain size.

#### References

- [1] BOMPAROLA R, CAPORALI S, LAVACCHI A, BARDI U. Silver electrodeposition from air and water-stable ionic liquid: An environmentally friendly alter native to cyanide baths [J]. *Surf Coat Technol*, 2007, 201(24): 9485–9490.
- [2] MASKII S, INOUE H, HONA H. Mirror-bright silver plating from a cyanide-free bath [J]. *Met Finish*, 1998, 96(1): 16–20.
- [3] CULJKOVIE J. Cyanide free bath for electro-deposition of silver: USA, 3984292 [P]. 1976–10–05.
- [4] LEAHY E P, KARUSTIS G A. Non-cyanide acidic silver electroplating bath and additive therefore: USA, 4067784 [P]. 1976–01–10.
- [5] SRIVEERARAGHAVAN S, KRISHNAN R M, NATARAJAN S R. Silver electro-deposition from thiosulfate solutions [J]. *Met Finish*, 1989, 87(7): 115–117.
- [6] NOBEL F I, BRASCH W R, DRAGO A J. Cyanide free plating solutions for monovalent metal: USA, 5302278 [P]. 1994–04–12.
- [7] JAYAKRISHNAN S, NATARAJAN S R, VASU K I. Alkaline noncyanide bath for electrodeposition of silver [J]. *Met Finish*, 1996, 94(5): 12–15.
- [8] SU Yong-tang, CHENG Dan-hong, LI Ke-jun, CAO Tie-hua, XU Wei-yi. Study on the thiosulfate cyanide-free silver pulse plating process [J]. *Plat Finish*, 2005, 27(2): 14–18. (in Chinese)
- [9] ANASTASSAKIS G, SEQUEIRA C A C. Electrochemical and surface analytical studies of silver deposits for industrial electroplating [J]. *Mater Sci Forum*, 2008, 587–588: 829–833.
- [10] ABBOTT A P, GRIFFITH J, NANDHRA S, O'CONNOR C, POSTLETHWAITE S, RYDER K S, SMITH E L. Sustained electroless deposition of metallic silver from a choline chloride-base dionic liquid [J]. *Surf Coat Technol*, 2008, 202(10): 2033–2039.
- [11] XIE Bu-gao, SUN Jian-jun, LIN Zhi-bin, CHEN Guo-nan. Electrodeposition of mirror-bright silver in cyanide-free bath containing uracil as complexing agent without a aeparate strike plating process [J]. *J Electrochem Soc*, 2009, 156(3): 79–83.
- [12] FISHELSON N, INBERG A, CROITORU N, SHACHAM-DIAMAND Y. Highly corrosion resistant bright silver metallization deposited from a neutral cyanide-free solution [J]. *Microelectron Eng*, 2012, 92: 126–129.
- [13] VALIUNIENEA A, BALTRUNASA G, VALIUNASA R, POPKIROV G. Investigation of the electroreduction of silver sulfite complexes by means of electrochemical FFT impedance spectroscopy [J]. *J Hazard Mater*, 210, 180(1–3): 259–263.
- [14] CAI X, BANGERT H. Hardness measurements of thin films-determining the critical ratio of depth to thickness using FEM [J]. *Thin Solid Films*, 1995, 264(1): 59–71.
- [15] WANG Shan-shan. Preparation of Ni, Ag, Cr films and study of their microstructure and mechanical properties [D]. Luoyang: Henan University of Science and Technology, 2011: 17–18. (in Chinese)
- [16] GUO Chang-lin, WU Yu-qin. An X-ray method of determining the degree of the preferred orientation of ferroelectric material with layer structure after hot-pressuring [J]. *Acta Phys Sinica*, 1980, 29(12): 1640–1644. (in Chinese)
- [17] REN Feng-zhang, ZHAO Shi-yang, LI Wu-hui, TIAN Bao-hong, YIN Li-tao, VOLINSKY A A. Theoretical explanation of Ag/Cu and Cu/Ni nanoscale multilayers softening [J]. *Mater Lett*, 2011, 65(1): 119–121.

## 硫代硫酸盐无氰镀银工艺及银镀层微观组织分析

任凤章<sup>1</sup>, 殷立涛<sup>1</sup>, 王姗姗<sup>2</sup>, A. A. VOLINSKY<sup>3</sup>, 田保红<sup>1</sup>

1. 河南科技大学 材料科学与工程学院, 洛阳 471023;

2. 洛阳轴研科技股份有限公司, 洛阳 471039;

3. Department of Mechanical Engineering, University of South Florida, Tampa, FL 33620, USA

**摘 要:** 采用硫代硫酸盐无氰镀银工艺, 分别以  $\text{AgNO}_3$  和  $\text{AgBr}$  为主盐进行镀银。研究主盐含量、电流密度对  $\text{Ag}$  镀层表面质量、沉积速率和显微硬度的影响, 并优化电镀参数。分析优化工艺下的  $\text{Ag}$  镀层结合强度和晶粒尺寸。结果表明: 在  $\text{AgNO}_3$  体系中,  $\text{AgNO}_3$  最佳用量为 40 g/L, 最佳电流密度为  $0.25 \text{ A/dm}^2$ , 制备的  $\text{Ag}$  镀层光亮平整, 与基体结合良好, 晶粒尺寸为 35 nm。在  $\text{AgBr}$  体系中的最佳  $\text{AgBr}$  用量为 30 g/L, 最佳电流密度为  $0.20 \text{ A/dm}^2$ , 与基体结合良好的  $\text{Ag}$  镀层的晶粒尺寸为 55 nm。与  $\text{AgBr}$  体系相比,  $\text{AgNO}_3$  体系适用的电镀电流密度范围较宽, 制备的  $\text{Ag}$  镀层显微硬度高, 晶粒尺寸小。

**关键词:** 无氰镀银; 硫代硫酸盐; 电流密度; 结合强度; 晶粒尺寸

(Edited by Chao WANG)